生化学 Biochemistry department

Medical Research Laboratories

岡山大学 OKAYAMA UNIV.

MASTER THESIS

Okayama University Graduate School of Medicine,
Dentistry and Pharmaceutical Sciences

Elucidating the role of ASAP1 in cancer invasion and correlation with Dynamin 2 in invadopodia formation

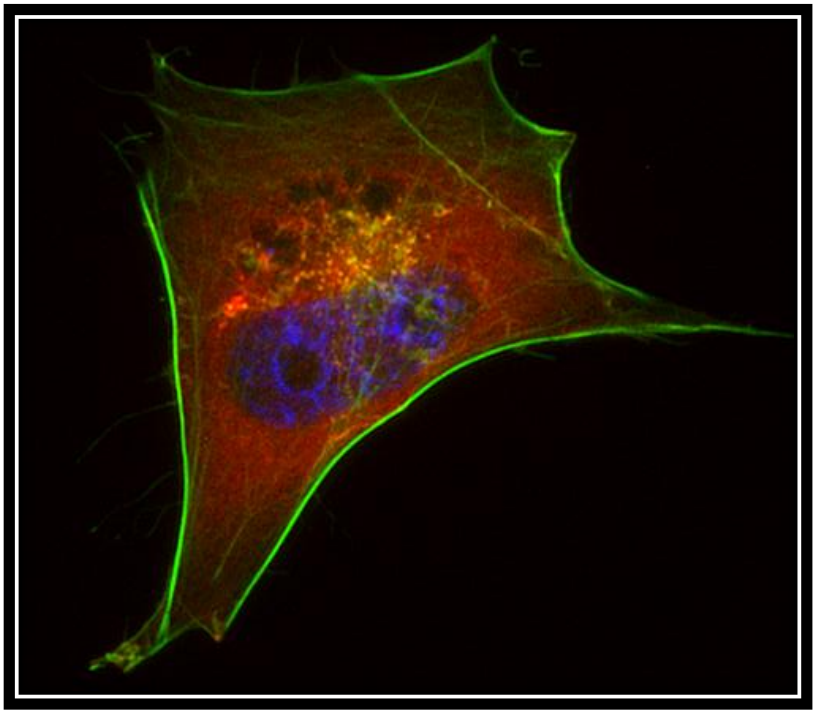

Federico Pratesi

Supervisor: Dr. Tetsuya Takeda

February 2017 – July 2017

Université Paul Sabatier TOULOUSE III

Biotechnologie Protéines Master Recombinantes

Acknowledgements

I would like to thank and express all my gratitude to Dr. Tetsuya Takeda, my supervisor and mentor, for the amazing opportunity to share time and experiences with him and all my colleagues at Okayama University. His guidance in the lab has always been very competent and useful not only for the techniques and strategies he taught me but also, and perhaps more importantly, for the scientific mindset that he is able to instill in his students. Takeda-Sensei will remain in my memories an example of a dedicated, dynamic, successful and funny scientist, extension of a truly rare good person.

A special acknowledgement is for my senpai and friend Kenshiro Fujise, a master 2 student like me, that has spent so much time and energy to help me and support me inside and outside the lab. Thank you for all the conversations, all the laughs, all the beers and in particular, your true friendship! I look forward to the day when we will open our own laboratory together.

I also need to thank Kohji Takei-Sensei, our P.I., for his constant presence inside and outside the lab. His patience during lab meetings and his experienced suggestions. For all the ice hockey training together and the barbecues he has promoted.

Many thanks to my amazing colleagues La-san, Wakita-chan, Ken-chan, Okamoto-kun and Sumida-san in the Biochemistry department for their practical and moral support and the days spent exploring Japan together.

I would like to thank my friends scattered around the globe for never leaving me alone and always be ready to make me smile, in particular Silvia, Jo, Amélie, Mary, Andre and all the others. You are my real treasure.

I also wish to especially thank Mélanie Chalvidan for her patience and support during all the six months of my internship and also for helping me change my path from Italy to France and now towards Canada; you are my strongest point and my life's best bet!

The last but not least acknowledgement is to my parents, the most important pieces in my personal history and the bravest people I have ever met! Without you, none of these wonderful experiences would have been possible and for this, and many other reasons, I cannot thank you enough. I will try my best to give you back some of the pride that you have made me feel during all these years.

Abstract

Cancer cell invasion is mediated by an actin-based membrane protrusion called invadopodia. This structure consists of an F-actin bundles core associated with proteolytic machinery and adhesive proteins that promote cell invasion by degrading extracellular matrix (ECM). Previous studies elucidated that dynamin 2 is required for invadopodia formation together with its binding partner cortactin, and plays crucial roles in cancer cell invasion. However, molecular network involved in the dynamin 2-dependent invadopodia formation remain to be elucidated.

The aim of my project is to elucidate the role of a possible partner of dynamin 2, ASAP1 (Arf-GAP with SH3 domain, ANK repeat and PH domain-containing protein 1), in cancer cell invasion. ASAP1, also called DDEF1, contains a membrane bending BAR domain and an SH3 (Src Homology 3) domain known to bind other proteins containing proline rich domains (PRD) such as dynamin 2. ASAP1 is also required for podosome assembly and ciliogenesis by regulating membrane trafficking and cytoskeletal organization. My research project consists of (1) examine localization of ASAP1 at the invadopodia in T24 (invasive bladder cancer cell line), (2) structure-function analyses of ASAP1 in invadopodia using truncations of ASAP1, (3) verification of the interaction between ASAP1 and dynamin 2, and (4) elucidating requirement of ASAP1 for invadopodia function by creating ASAP1 KD (knock down) stable cell line with shRNA for ASAP1. My research showed for the first time that ASAP1 functions at the invadopodia of bladder cancer cells together with dynamin 2.

Glossary

Arf: ADP ribosylation factor

Arp2/3: Actin-Related Proteins 2/3

ASAP1: Arf-GAP with SH3 domain, ANK repeat and PH domain-containing protein 1

BAR: Bin, Amphiphysin and Rvs

CO2: Carbon dioxide

DMEM: Dulbecco modified eagle medium

DNA: Deoxyribonucleic acid

ECM: extracellular matrix

EDTA: Ethylenediaminetetraacetic acid

EGFP: Enhanced Green Fluorescent Protein

FBS: fetal bovine serum

GED: GTPase effector domain

GST: Glutathione Sepharose Trap

GTP: guanosintrifosfato

HEK293T: human embryonic kidney 293 T antigen

IgG: immunoglobulin G

KD: knock down

LB: Lysogeny broth

MCF7: Michigan Cancer Foundation-7

mRFP: monomeric red fluorescent protein

MT1-MMP: Membrane type 1 metalloprotease

$NaBH_4$: Sodium borohydride

NaCl: Sodium chloride

PBS-T: Phosphate Buffered Saline with Tween

PCR: Polymerase chain reaction

PH: Pleckstrin homology

PMSF: phenylmethylsulfonyl fluoride

PRD: proline rich domain

P/S: penicillin/streptomycin

RC: radical cystectomy

RNAi: Ribonucleic acid interference

RPMI: Roswell Park Memorial Institute

SDS-PAGE: Sodium Dodecyl Sulfate Polyacrylamide Gel Electrophoresis

SH3: SRC Homology 3

shRNA: short hairpin RNA

SOC: Super Optimal Broth

SV-HUC-1: SV40-immortalized human uroepithelial cell

WASP: Wiskott–Aldrich syndrome protein

WIP: WASP-interacting protein

Table of contents

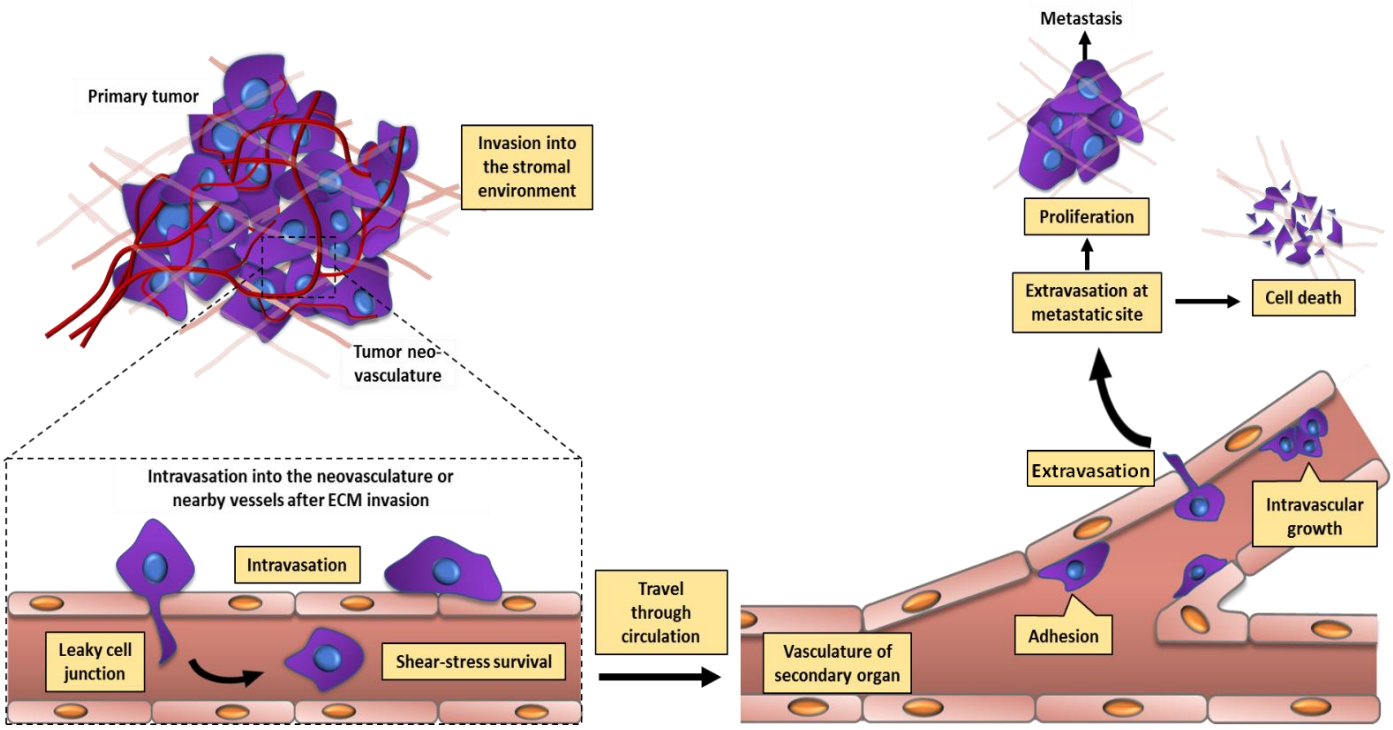

Figure 1: Cancer cells invasion and metastasis. Primary tumor forms new blood vessels in a process called angiogenesis. If not treated, the cells can detach the cancer mass and start to invade the stromal environment surrounding the area. Once they reach a blood vessel, they can start the intravasation and leak into the blood stream; if the cancer cell survives the immune cells in the blood stream after traveling through the circulation system, they are able to adhere to the blood vessel and invade new areas and create metastasis or start an intravascular growth. Once in the secondary tumor site, they can proliferate or succumb to the immune system and encounter cell death [1, 3, 32].

I. Introduction

Cancer cells can be distinguished by their unique ability to spread throughout the body by two related mechanisms: invasion and metastasis [1] (Figure 1). After the growth of the primary tumor, the cells on the edge of the cancer mass can extend and form protrusion capable of invading neighboring tissues [1]. The proliferation of transformed cells and the increased volume of the tumor eventually leads to a breach in the barriers between tissues and the start of the true cancer invasion [2]. During this process, secondary tumor sites or metastasis are formed. The "metastatic cascade" is the term that describe the orderly process that leads the cancer cells to create new tumor masses in other regions of the body after penetrating the lymphatic or blood vessels [3]. This intravasation is also facilitated by the angiogenesis process, which can develop, following stimulation of endothelial cells, a new vascular network near the tumor, providing a blood supply for the cancer mass [2,3]. More a cancer is capable to invade, more aggressive will be the disease and weaker the survival rate [4].

Among the known aggressive cancers, bladder cancer is the second most common urological cancer worldwide with a 70% recurrence rate after surgery of superficial (non-muscle invasive) stage [5,6]. The primary option for the muscle-invasive bladder cancer remains radical cystectomy (RC), a procedure that cures approximately 2/3 of patients [7]. Unfortunately, quality of life of patients and their caregivers is significantly affected after RC and social healthcare system suffers from this heavy burden [8]. Thus, alternative approaches that will efficiently restrict bladder cancer cells within their original local lesion for subsequent non-radical treatments need to be developed.

Tumor invasion is mediated by the ability of cancer cells to form actin-based membrane protrusion called invadopodia (Figure 2) [9]. This structure consists of an F-actin bundles and it is essential for promotion of cell invasion by degrading extracellular matrix (ECM). Invadopodia exhibit three core neoplastic functions associated with malignancy: invasiveness (requiring F-actin, Arp2/3, WASP/WIP, cortactin), adhesion (requiring α/β integrins) and proteolysis (requiring MT1-MMP and MMP2/9) [9, 10]. Not only they help for the penetration of basement membrane, but invadopodia also participate in essential steps of stromal invasion, intravasation, extravasation and lethal distant metastasis [11]. Thus, inhibition of invadopodia formation and/or function has promise for the therapeutic suppression of cancer cell invasion and metastasis.

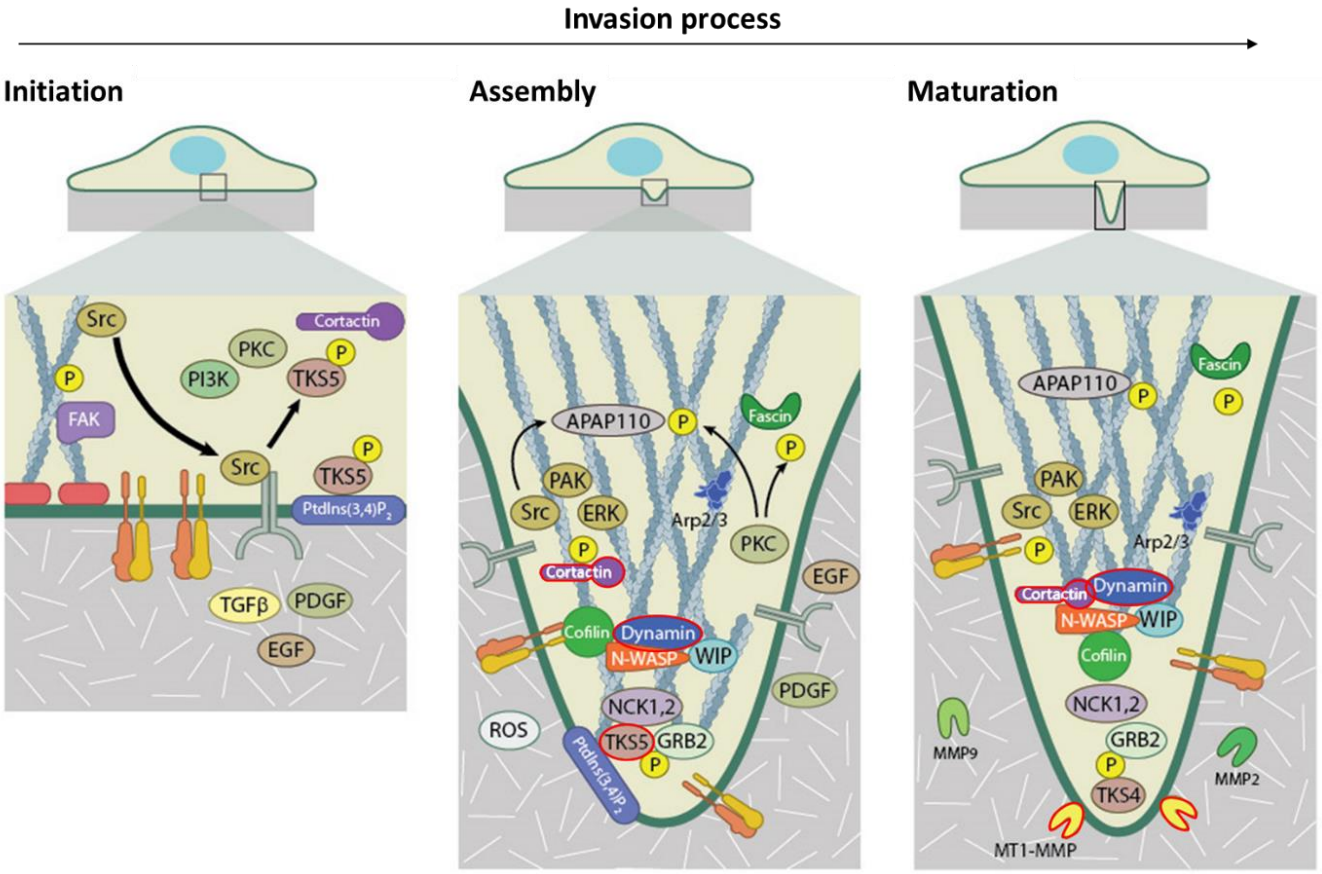

Figure 2: Invasion process by invadopodia maturation. Molecular machinery inside the invadopodia during the maturation process. Many molecules and proteins are responsible for the invadopodia formation. Among them Actin, Cortactin and Dynamin are well characterized. Other partners in the process are the adapter protein TKS5 and the metalloprotease MT1-MMP. The proteins contained in the invadopodia can form complexes that facilitate the transport of proteinase and proteolytic molecules at the edge of the structure to digest the ECM. Other proteins can create internal structures, such as actin bundles, to stabilize the invadopodia and enhance the invasion ability. The image was modified from [33].

Another important player in invadopodia formation and function is dynamin, a large GTPase essential for membrane fission in clathrin-mediated endocytosis [12]. Three different dynamin isoforms are found in mammalian cells: dynamin 1 (neuronal isoform), dynamin 2 (ubiquitous isoform) and dynamin 3 (a testis, lung and brain isoform) [13]. All the dynamin isoforms share similar domain structures aligned from N-terminus to C-terminus: a GTPase domain, a middle domain, a PH domain, a GTPase effector domain (GED) and PRD (Figure 3) [13]. Dynamin is also known to regulate the actin cytoskeleton either directly or indirectly via interaction with various actin-binding proteins such as cortactin (Figure 2). Dynamin2 has been implicated in the regulation of invasiveness and invadopodia formation in lung cancer cells [14], highly invasive melanoma cells [15] and bladder cancer cells [12]. However, molecular networks involved in the dynamin 2-mediated invadopodia formation remains to be elucidated.

ASAP1 is a BAR domain protein and a potential regulator of membrane remodelling during cancer invasion [16, 17]. Although its function in cancer invasion is not well understood, the presence of a membrane bending BAR domain and an SH3 domain in its C-terminal, known to be able of binding with a proline-rich domain which is present in the dynamin 2 (Figure 3), have made ASAP1 as a good candidate for a binding partner of dynamin 2 in the invadopodia formation [17, 18]. ASAP1 has a molecular mass of 130 KDa and it is localized in the cytoplasm, and the membrane at the leading edge [19]. ASAP1 has a role as GTPase-activating protein for Arf (ADP ribosylation factor) family proteins and it is also responsible for various essential processes such as podosomes assembly and ciliogenesis via regulating membrane trafficking and cytoskeletal remodelling [18, 19]. Involvement of ASAP1 in ciliogenesis was very interesting since invadopodia and cilia are both membranous protrusion to the extracellular space [16]. There is also a correlation between dynamin 2 and ASAP1 in podosome assembly and invadopodia formation: both proteins are implicated in intracellular transport, they interact with actin filaments, they can link cortactin and paxillin (important invadopodia/podosomes markers), they collaborate in podosomes formation in normal migration and they both interact with Src (proto oncogene) [12, 14, 15, 16]. All these clues motivated us to elucidate possible function of ASAP1 at invadopodia in correlation with the activity of dynamin 2 in cancer cell invasion.

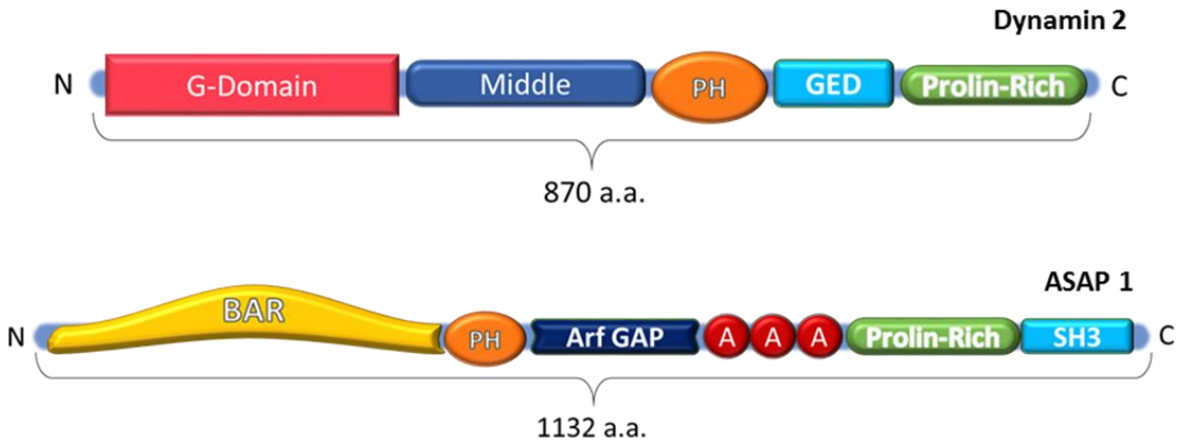

Figure 3: Primary structure of Dynamin 2 and ASAP1. Dynamin 2 is composed of a GTP domain capable of binding and hydrolyse GTP; a middle domain, critical for tetramerization and higher-order self-assembly; PH domain, implicated in the mediation of protein-protein and protein-phospholipid interactions; GED domain, essential for self-assembly and stimulation of GTPase activity and proline-rich domain, an SH3-binding domain.

ASAP1 contains a BAR domain, wich is banana shaped and binds to membrane via its concave face and capable of sensing membrane curvature by binding preferentially to curved membranes; PH domain, implicated in protein-phospholipid interactions ; Arf GAP domain, important for the hydrolysis of GTP to GDP to transition Arf from the active, GTP bound, state to the inactive, GDP bound, state; Ankyrin repeat, is one of the most common protein–protein interaction motifs in nature; proline-rich domain, an SH3-binding domain and an SH3 domain, known to interact with adaptor proteins and tyrosine kinases.

In this study, I examined (1) localization of ASAP1 at the invadopodia, and its co-localization with dynamin 2, (2) structure-function relationships of ASAP1 in invadopodia using truncations of ASAP1, (3) interaction between dynamin 2 and ASAP1 using biochemical approaches, and (4) the requirement of ASAP1 in invadopodia function exploiting RNAi technology.

II. Materials and methods

Cell culture

SV40 immortalized transitional epithelium cell line SV-HUC-1 (ATCC No. CRL-9520) was obtained from RIKEN BRC, transitional cell carcinoma T24 (ATCC No. HTB-4) was obtained from ATCC, MCF7 and MDA-MB-231 from Dr. Hideki Yamaguchi (Sasaki Foundation, Japan). SV-HUC-1, T24 and MCF7 were cultured in RPMI-1640 medium (Wako Pure Chemical Industries) supplemented with 10% fetal bovine serum (FBS) and 1% penicillin/streptomycin (P/S), MDA-MB-231 cells were cultured in DMEM (Wako Pure Chemical Industries) and RPMI-1640 mix in 1:1 ratio (10% FBS and 1% P/S) at 37 °C in humidified air with 5% CO2.

Reagents

Polyclonal goat anti-dynamin 2 antibody (Sc-6400) was purchased from Santa Cruz Biotechnology, monoclonal mouse anti-cortactin antibody (05-180, clone 4F11) was purchased from Millipore, and monoclonal mouse anti FLAG (F1804) was from Sigma-Aldrich. HRP conjugated goat anti-Rabbit IgG (H +L) (31460), rabbit anti-mouse IgG (H + L) (31450) and rabbit anti-goat IgG (H + L) (31402) secondary antibodies were purchased from Thermo Fisher Scientific. Thermo Fisher Scientific also supplied Alexa conjugated secondary antibodies including Alexa Fluor 350 conjugate goat anti-rabbit IgG (H + L) (A-11046), Alexa Fluor 488 conjugate donkey anti-goat IgG (H + L) (A-11055), Alexa Fluor 546 conjugate donkey anti-goat IgG (H + L) (A-11056), Alexa Fluor 555 conjugate donkey anti-mouse IgG (H + L) (A-31570), Alexa Fluor 488 conjugate goat anti-mouse IgG (H+ L) (A-11001), Alexa Fluor 555 Phalloidin (A34055) and Alexa Fluor 488 Phalloidin (A12379).

DNA cloning and mutagenesis

Gateway cloning technology (Thermo Fisher Scientific) was used for DNA cloning. Entry clones of full length and BAR domain only truncation of ASAP1 were gifts from Harvey McMahon (MRC-LMB, UK). ΔSH3 truncations of ASAP1 was amplified by PCR (Polymerase chain reaction) using full length ASAP1 as a template with the following primers: 5'-GGGGACAAGTTTGTACAAAAAAGCAGGCTGCatgagatcttcagcctccaggc-3' and 5'-GGGGACCACTTTGTACAAGAAAGCTGGGTCtttccccgtattgatttttctg-3' (small caps are gene specific sequences and capitals are sites for recombination used in Gateway cloning) and resultant PCR product was cloned into pDONOR201 vector by BP reaction to prepare Entry clones. Entry clones of full length, BAR domain only and SH3 deletion of ASAP1 were used for LR reaction with destination vectors to prepare expression constructs for GFP-, mRFP- and FLAG-tagged proteins.

Plasmids amplification and purification

HiSpeed Plasmid Midi Kit (Qiagen) was used following manufacturer's instruction. Briefly, 50 µl of competent bacteria (Top10, Thermo Fisher) were transformed with 2 µl of plasmid for 30 min at 4°C, heat shocked at 42°c for 30 seconds followed by incubation for 30 minutes at 37°C in 150 µl of SOC medium. All the mixture was spread on petri dish with 100 µg/ml of Ampicillin and incubated at 37°C overnight. One colony was picked and inoculated in 50 ml of LB medium with 100 µg/ml of Ampicillin and incubated at 37°C overnight under agitation. Plasmids were then purified from the overnight culture following the instruction manual. After purification, purity and concentration of the plasmid was analyzed by spectrophotometer (Ultraspec 3100 pro, Amersham Biosciences).

Immunoblotting

SDS-PAGE samples were prepared from cell extracts of either HEK293T or T24 cells and separated using Mini-PROTEAN System (Bio-Rad). Separated proteins were transferred to nitrocellulose blotting membrane (Amersham Protran Premium 0.45 mmNC, GE Healthcare Life Sciences) using Mini Trans-Blot Cell (Bio-Rad). Membranes were blocked in blocking buffer (PBS-T with 3% skimmed milk) for 1 h at room temperature before incubation with primary antibodies diluted in the blocking buffer (1:1000 for ab52611, sc-6400 and PA1-662; 1:10000 for A5441) overnight at 4°C. After washing three times in blocking buffer, membranes were probed with HRP-conjugated secondary antibodies (1:5000 in dilution) for 1 h at room

temperature before signal detection by Amersham ECL Prime Western Blotting Detection Reagent (RPN2232, GE Healthcare) with ChemiDoc Touch Imaging System (Bio-Rad).

Transfection of expression constructs

LTX lipofectamine and Plus reagents (Invitrogen) were used following manufacturer's instruction. Normally, for each transfection in a 6 wells plate were used 250 µl of Opti-MEM medium, 2.5 µl of PLUS reagent, 7.5 µl of LTX and 2.5 µg of DNA.

Transfection of shRNA constructs

shRNAs were transfected into the cells using LTX lipofectamine and Plus reagents (Invitrogen) following manufacturer's instruction. Two negative controls, shRNA anti Firefly Luciferase (gift from Harvey McMahon, MRC-LMB) and shRNA MISSION anti target (from Sigma-Aldrich) were used in this study. Nine shRNAs against genes: shRNA against ASAP1.1, ASAP1.2, ASAP1.3, MISSION shRNA (from Sigma-Aldrich) against ASAP1.1, ASAP1.2, ASAP1.3; MISSION shRNA against Dynamin2.1, Dynamin2.2, Dynamin2.3. Selection has been made by increasing the concentration of Puromicyn (from Sigma-Aldrich) from 0.5 µg/ml up to 30µg/ml in three weeks.

Invadopodia induction assay

To induce invadopodia formation, gelatin-coated coverslips were prepared as previously described [21] with the following modifications. In short, acid washed coverslips were coated with 2.5% porcine skin gelatin (Sigma-Aldrich) and incubated on ice for 30 minutes on a drop of 0.5% glutaraldehyde, then aldehyde base was quenched in 5 mg/mL $NaBH_4$ with gentle washing with 1x PBS between each step. The gelatin-coated coverslips were then sterilized in 70% ethanol for 30 minutes, washed in autoclaved 1x PBS and soaked in RPMI-1640 medium or mix RPMI-1640 and DMEM (1:1 ratio) for 1 h before using. T24, MCF7 and MDA-MB-231 cells were detached with trypsin-EDTA, seeded onto the prepared gelatin-coated coverslips and incubated in the correct media for 8 h prior to microscopic imaging.

Immunofluorescence microscopy:

Cells attached to coverslips were fixed with 4% paraformaldehyde in PBS for 15 min at room temperature. After blocking and permeabilization in PBS with 3% BSA and 0.5% TX-100

for 1 h at room temperature, the fixed cells were probed with primary antibodies diluted in antibody buffer (PBS with 1% BSA and 0.1% TX-100) overnight at 4°C. After washing in the antibody buffer, the cells were probed with Alexa-conjugated secondary antibodies diluted in the antibody buffer (1:1000) for 3 h at room temperature. Treated coverslips were mounted on microscope slides (Matsunami) using Fluoromount/Plus (K048, Diagnostic BioSystems) and images were captured on a fluorescence equipped BX51 (Olympus) microscope fitted with cMOS CCD camera (Tucsen MH-15), or captured on a laser scanning confocal microscope (Zeiss LSM-780). Images were analyzed and processed with ImageJ software (National Institutes of Health).

Co immuno precipitation (Co-IP) assay

Preparation of cell lysate: after cell culture of T24 for 48h after transfection in 6 well plate and reached confluence, the medium was aspirated and transfer in a 15 ml falcon tube for centrifugation (2000 g at 4°C for 5 minutes). During this time 400 µl of extraction buffer (20 mM HEPES, 150 mM NaCl, 1 mM EDTA, 0.2% Triton X-100, 0.1 mM PMSF, 1 tablet of cOmplete^{TM} proteinase inhibitor) were add in each well and kept on ice. After centrifugation, the extraction buffer was then used to resuspend the attached cells into the wells and aspirate to resuspend the pellet in the falcon tube. Sonication was used to lyse cells and centrifuged at 15000 g in the Eppendorf tube for 10 minutes at 4°C. The resultant supernatant was then transferred in a new tube and 10 µl of Anti-FLAG M2 magnetic beads (Sigma-Aldrich) were used to immunoprecipitate FLAG-tagged ASAP1 fragments. Three washing steps were performed with the extraction buffer before sample preparation for Western Blot.

Visual Immuno Precipitation (VIP) assay

T24 cells, cultured in RPMI-1640 medium supplemented with 10% fetal bovine serum and 1% P/S, were plated in 6 well plates. Cells at approximately 90% confluency were transfected with EGFP and mRFP fusion constructs using lipofectamine LTX and PLUS reagent (Invitrogen) following manufacturer's instruction, and then cultured for 48 h. Before the assay, expression of fluorescent fusion proteins was confirmed under a fluorescence microscope. The cells were lysed in 400 µl of lysis buffer (20 mM HEPES-KOH pH 7.4, 150 mM NaCl, 0.1% Triton X-100 and 10% glycerol, with cOmplete protease inhibitor cocktail). After 15 min on ice, the cell lysates were centrifuged at 16000 g for 15 min at 4°C in a microcentrifuge. The supernatants (350 µl)

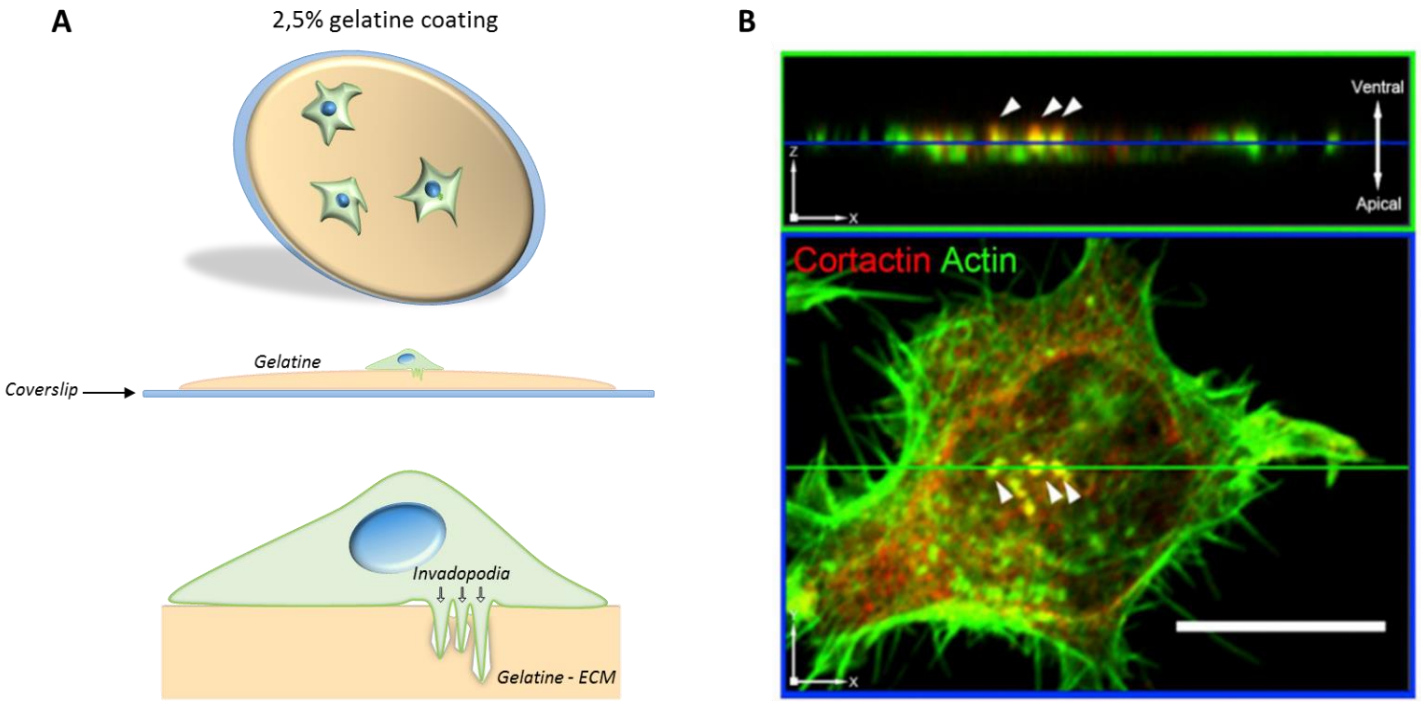

Figure 4. Invadopodia induction assay: gelatine coated coverslips. (A) Acid washed 12 mm coverslips were coated with 2,5% gelatine solution. After sterilization and incubation with the correct medium, cells were cultured for 8h to induce invadopodia and better imaging them under the microscope. (B) Previous experiments using this invasion assay and the T24 cell line [12], has been used to characterize invadopodia in this specific cancer cell line. Confocal microscopic image of T24 cells stained to reveal 3-D localization of cortactin (red) and actin (green) at invadopodia. Note that actin and cortactin colocalize on the protrusions aligned on the ventral cell surface (arrowheads). The image was adapted from [12].

were incubated with 30 µl of GST-tagged anti-GFP nanobody pre-bound to glutathione–sepharose 4B beads (GE Healthcare Life Sciences) in 1.5 ml Eppendorf tube for 1 h at 4°C by rotation. The tubes were centrifuged at 2000 g for 30 s at room temperature. The precipitated beads were washed three times with 200 µl of lysis buffer, and then transferred on a microscope slide for observation. Fluorescence on the beads was observed using fluorescence equipped BX51 (Olympus) microscope fitted with cMOS CCD camera (Tucsen MH-15) using a 10× objective lens under fixed conditions (for green fluorescence, sensitivity ISO 400, exposure 0.25 s; and for red fluorescence, sensitivity ISO 800, exposure 1.25 s). Image acquisition was performed under fixed conditions. The quantification of fluorescence intensity was performed using the ImageJ software (National Institutes of Health).

III. Results and discussion

Optimization of invadopodia induction assay

Invadopodia are invasive structures used by cancer cells to degrade the ECM and migrate to reach other tissues and/or organs [20, 22]. For the better reproduction of this phenomenon *in vitro*, I thought to simulate the ECM texture using a thin layer of gelatine and coat coverslips with it. The protocol was adapted from the ones previously used in our lab or by another team [12, 21]. After a few trials to improve the technique and condition of cell culturing, I found that 8 h seeding was the optimal condition for cells to be analysed after fixation. This protocol was used as an invasion assay (Figure 4 A) and, in a precedent study in our laboratory, was used to characterize invadopodia in T24 cells using invadopodia markers such as cortactin and actin (Figure 4 B) [12].

Localization of ASAP1 at invadopodia in T24

Previous studies showed the presence of ASAP1 in invadopodia in other type of cancer cells [23, 25], but my goal at this stage was to prove the localization of ASAP1 at invadopodia in the bladder cancer cell line T24. Since we didn't have a specific antibody for ASAP1 to analyse endogenous proteins, we prepared GFP-tagged, mRFP-tagged and FLAG-tagged version of ASAP1 using Gateway cloning system and used them for further experiments. To confirm the presence of ASAP1 at invadopodia in T24, localization of ASAP1 was analysed by immunofluorescence microscopy using the FLAG-tagged ASAP1 (Figure 5A). The invadopodia

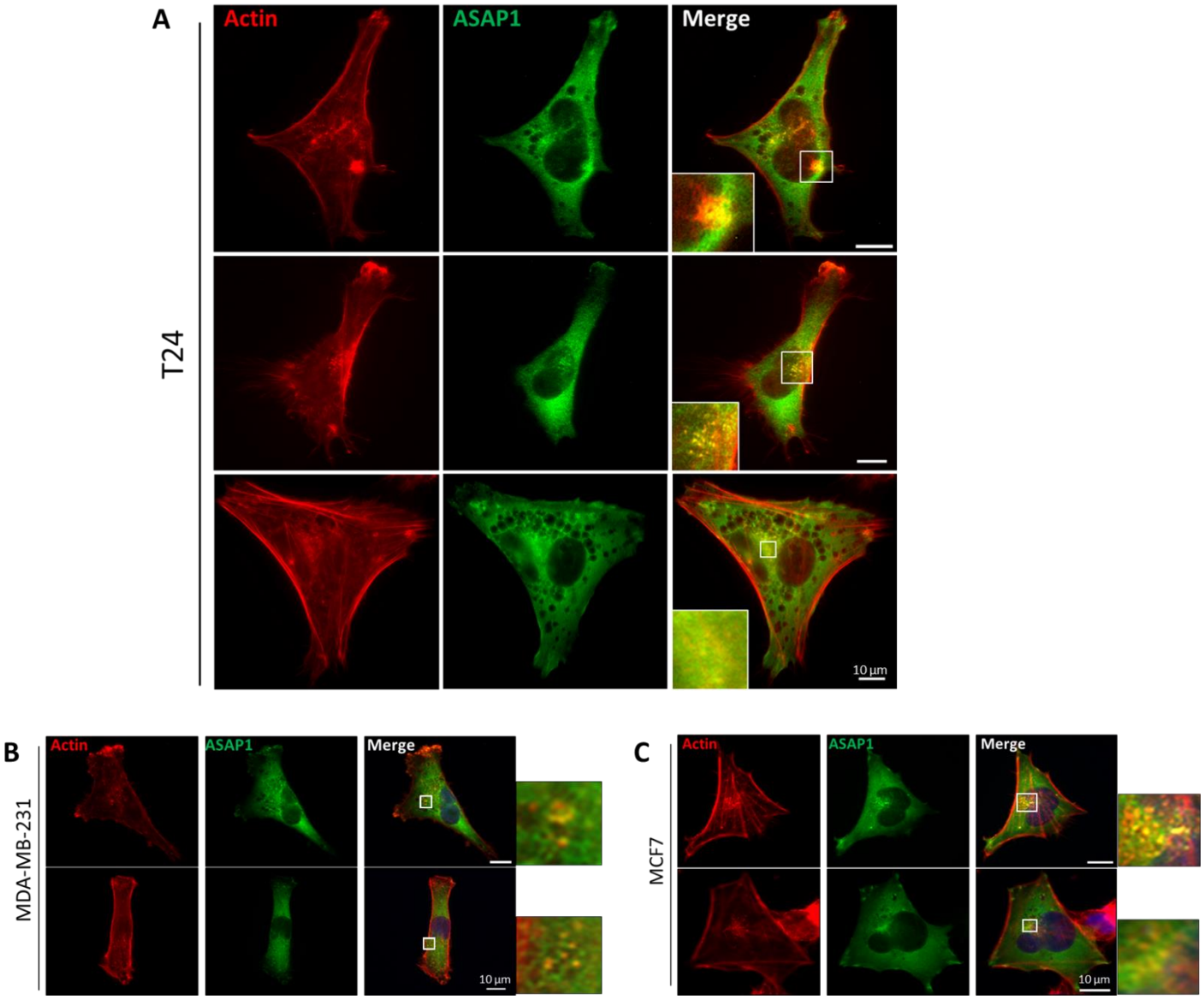

Figure 5. Localization of ASAP1 at invadopodia. Immunostaining for actin (red) and ASAP1-FLAG (green), shows the co-localization of these proteins at the actin enriched invadopodia. (A) T24 cells show different phenotype associated with cell invasion on the gelatine coating. (B) MDA-MB-231 and (C) MCF7 are used as control to show a similar invasive phenotype as puncta cluster. The co-localization of ASAP1 and actin in all the samples is suggesting a potential role of ASAP1 in these three cancer cell invasion processes.

were clearly clustered at the perinuclear area in T24 as confirmed by F-actin staining with phalloidin (Figure 5 A, Actin). Different structures of invadopodia were observed, such as big concentrated spots (Figure 5 A, first lane), punctated clusters (Figure 5 A, second lane) and scattered dots (Figure 5 A, third lane). ASAP1 was co-localized with actin at the invadopodia in all of these structures giving us a clue to characterize this protein in the invadopodia (Figure 5 A, ASAP1). I also examined localization of ASAP1 in two other invasive cancer cell lines, MDA-MB-231, an aggressive breast cancer cell line, and MCF7, a less aggressive breast cancer cell line. Our invasion assay with gelatine coated coverslips induced invadopodia with actin in both breast cancer cell lines (Figure 5 B and C, Actin) and localization of ASAP1 in invadopodia was also easily spotted (Figure 5 B and C, ASAP1). Taken together, all these clues suggested that ASAP1 could be a component of invadopodia in various cancer cells.

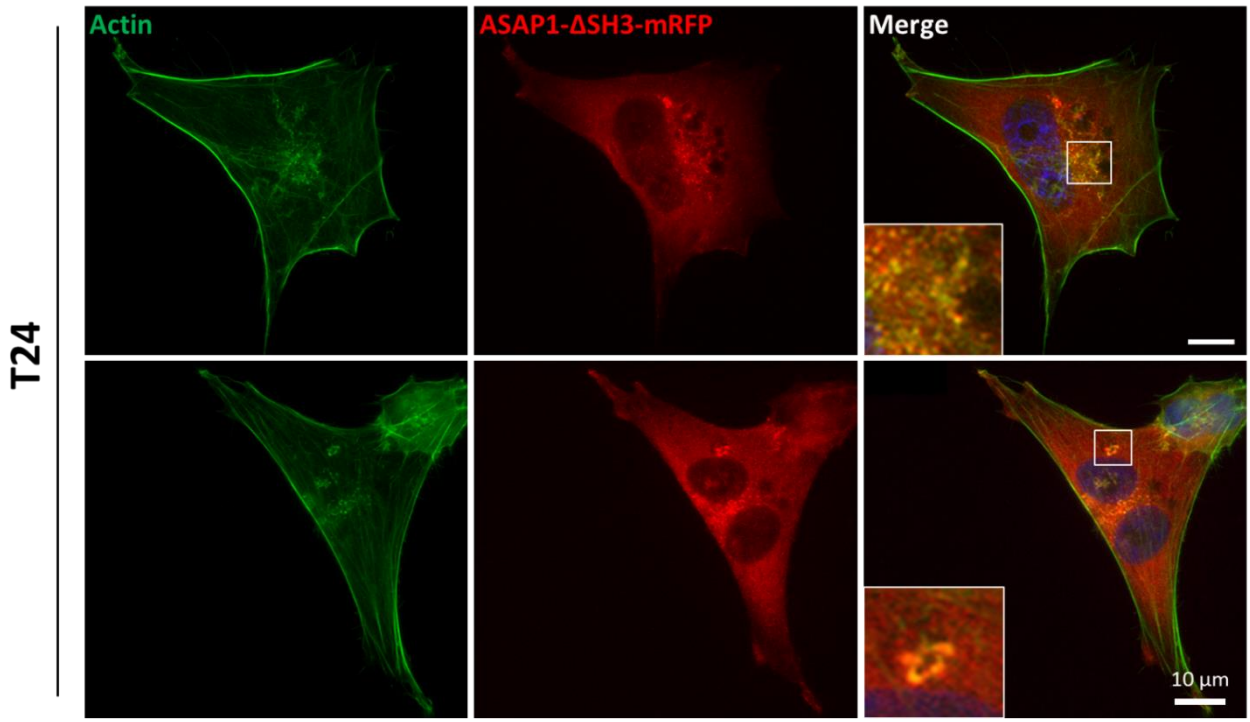

Figure 6. Localization of ASAP1-ΔSH3 at invadopodia. Immunostaining for actin (green) and ASAP1--ΔSH3-mRFP (red), shows the co-localization of these proteins at the actin enriched invadopodia. No significant changes in the ASAP1 truncated sequence localization inside the cell can be detected. In the second lane, a rosetta structure can be seen.

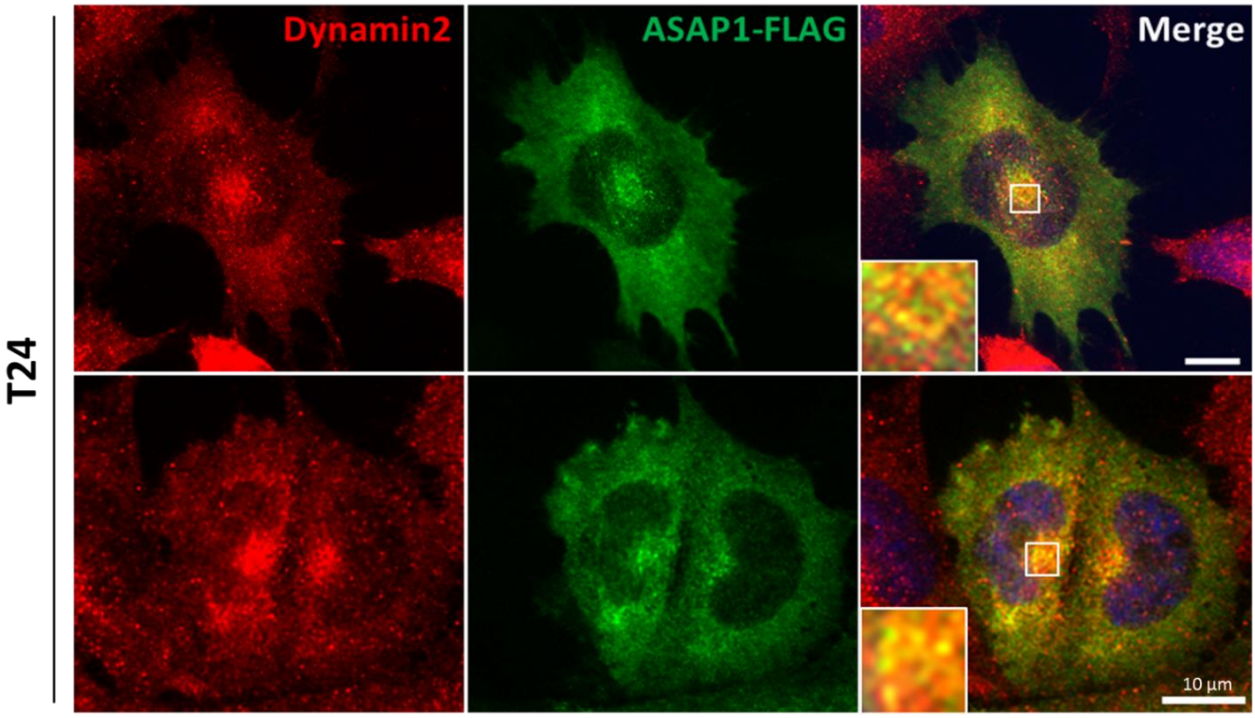

Figure 7. Co-localization of ASAP1 and Dynamin 2 at invadopodia. Immunostaining of T24 cells for dynamin 2 (red) and ASAP1 (green), shows the co-localization of these proteins at the invadopodia.

Structure-function analyses of ASAP1 in invadopodia

Next, I performed structure-function analyses of ASAP1 by examining localization of various truncations of ASAP1. The first truncation of ASAP1 used was the one containing only BAR domain (ASAP1-BAR) which has the ability to bend the membranes [26]. ASAP1-BAR localized in the cytoplasm and at filopodia, but not to the invadopodia (data not shown). In contrast, another truncation in which C-terminal SH3 domain was deleted (ASAP1-ΔSH3) localized to the invadopodia (Figure 6, first lane, ASAP1-ΔSH3-mRFP) together with actin (Figure 6, first lane, Actin). Taken these results together, we assumed that key regions responsible for localizing ASAP1 to the invadopodia should exist between the BAR domain and the SH3 domain. Interestingly, ASAP1-ΔSH3 also localized to a circular structure so called rosetta which is a peculiar invadopodia organization [10, 20, 27] (Figure 6, second lane). This particular rosetta organization shows a normal phenotype of invadopodia maturation even with the overexpression of ASAP1-ΔSH3. There is no negative effect on invadopodia formation and organisation by the expression of either ASAP1-BAR or ASAP1-ΔSH3, but only localization was affected.

Co-localization of ASAP1 and dynamin 2 at invadopodia

I then examined co-localization of ASAP1 and dynamin 2 at the invadopodia. Endogenous dynamin 2 localized to the invadopodia as previously shown [12] (Figure 7, Dynamin 2). ASAP1-FLAG constructs transfected to T24 cells co-localized with dynamin2 at the invadopodia at the perinuclear region (Figure 7, ASAP1-FLAG). These results suggest that dynamin 2 and ASAP1 cooperatively function at the invadopodia in the invasive cancer cells. Dynamin 2 and ASAP1 were also co-localized in the invadopodia of breast cancer cell line MDA-MB-231 and MCF7 (data not shown), suggesting a solid constancy about cooperative function of ASAP1 and dynamin 2 in different type of cancers. Further experiments with other cancer cell types using confocal microscopy will clarify detailed spatial distribution of dynamin 2 and ASAP1 in the invadopodia.

Verification of the interaction between ASAP1 and dynamin 2

For a better understanding of the cooperative function of ASAP1 and dynamin 2 at the invadopodia, I examined their interaction using three different biochemical approaches. The first experiment was a co-immunoprecipitation (co-IP) assay. For the co-IP experiment, I used HEK-293T cells in the first place because of its high transfection efficiency and high level of

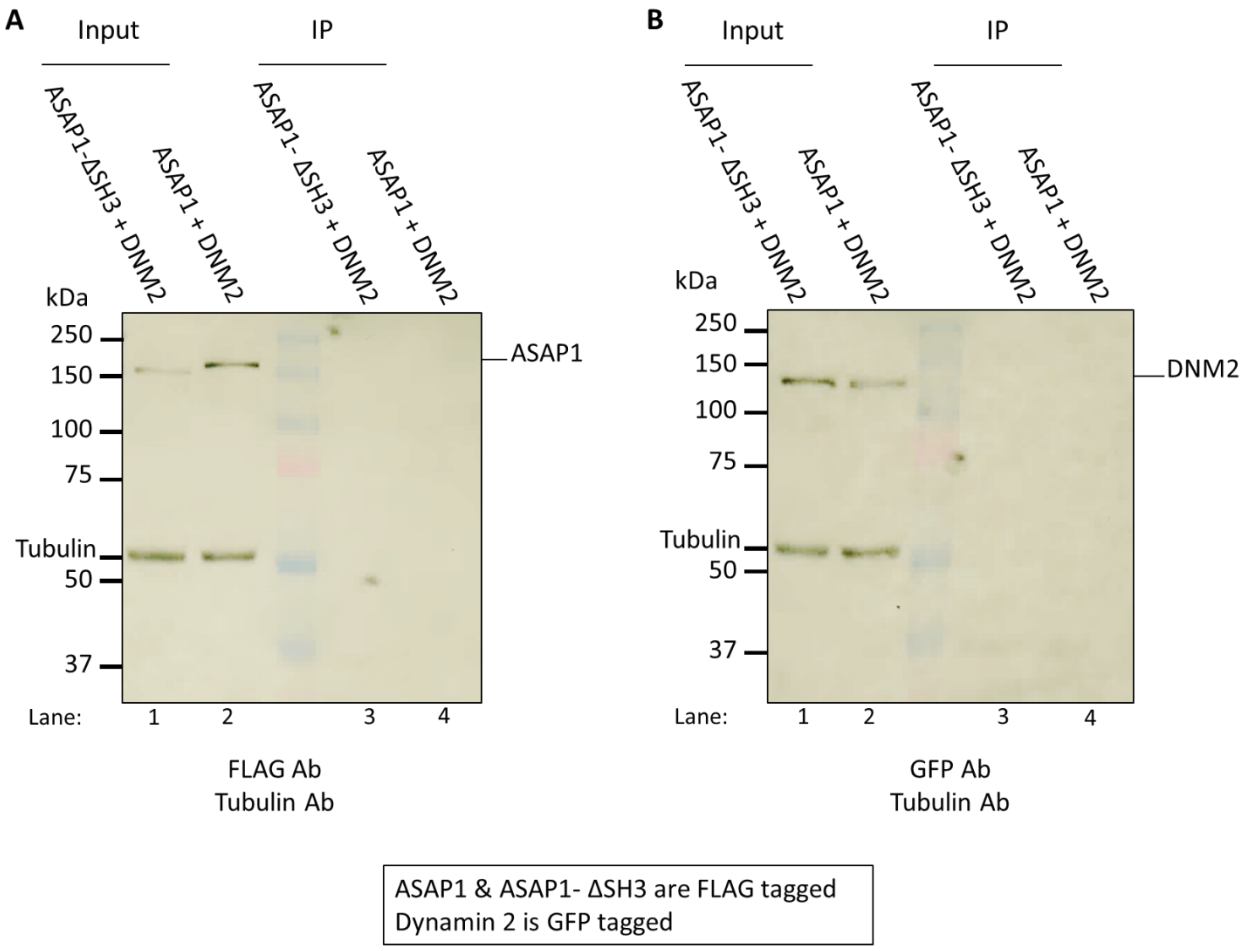

Figure 8: Co-immunoprecipitation of dynamin 2 GFP tagged and ASAP1 FLAG tagged. (A) The membrane shows the presence in the input sample of the truncated version of ASAP1-ΔSH3 (lane 1) and the full-length protein (lane 2). After immunoprecipitation, no signal of the FLAG tagged ASAP1 proteins is detectable meaning no interaction with dynamin 2. (B) Confirmed presence on the membrane of the dynamin 2 in the input samples. Unfortunately, after the immunoprecipitation the protein GFP tagged is not detectable showing a probable flaw in the protocol.

protein expression [28]. Unfortunately, the cell culturing and protein production were not very satisfying in the first two attempts (low number of cells after 60 hours and low amount of protein expression) so I decided to use T24 cells instead. The T24 cells were suitable for a large-scale transfection, a necessity for compensating their low transfection efficiency, and they reached to full confluency in just 36-48 hours after transfection when they were seeded at 80% confluency at the day 1. After collecting all the cells, sonicate them and centrifugate the solution to collect only the proteins contained, I prepared the input samples to run later on the SDS-PAGE gel. The rest of the protein solution was used to perform the co-IP experiment hoping to catch FLAG tagged ASAP1-BAR (negative control for interaction) and ASAP1 with the nanobeads and their associating proteins, in our assumption GFP tagged dynamin 2. After the incubation and washing steps, I run the input and after co-IP samples on the same gel in two copies, one to detect with the anti-FLAG antibody and the other to detect with the anti-GFP antibody by western blot analysis. Unfortunately, ASAP1-BAR domain didn't express enough and all the attempts to obtain a solid result failed (data not shown).

I then moved to a pull-down assay using purified GST-nanobody anti-GFP bound to glutathione-sepharose 4B beads. This experiment was performed to obtain a better result using the reverse catch strategy in which GFP-tagged dynamin 2 was immunoprecipitated to pull down a putative interactor, FLAG-tagged ASAP1. To avoid the poor expression problem of ASAP1-BAR, I decided to switch the control to the SH3-truncated form of ASAP1 (ASAP1-ΔSH3), legitimizing my choice knowing that the possible dynamin 2 binding domain in ASAP1 was the SH3 domain [29]. In this case, FLAG-tagged full-length ASAP1 or ASAP1-ΔSH3 (Figure 8 A, lane 1 and 2) and GFP-tagged dynamin2 (Figure 8 B, lane 1 and 2) were co-expressed in T24. However, signals of the target proteins could not be detected after pull-down and it was impossible to confirm or deny the presence of the proteins or their interaction (Figure 8 A and B, lane 3 and 4). I repeated experiments several times trying to optimize the experimental condition and my technical performance, but no clear improvement was achieved.

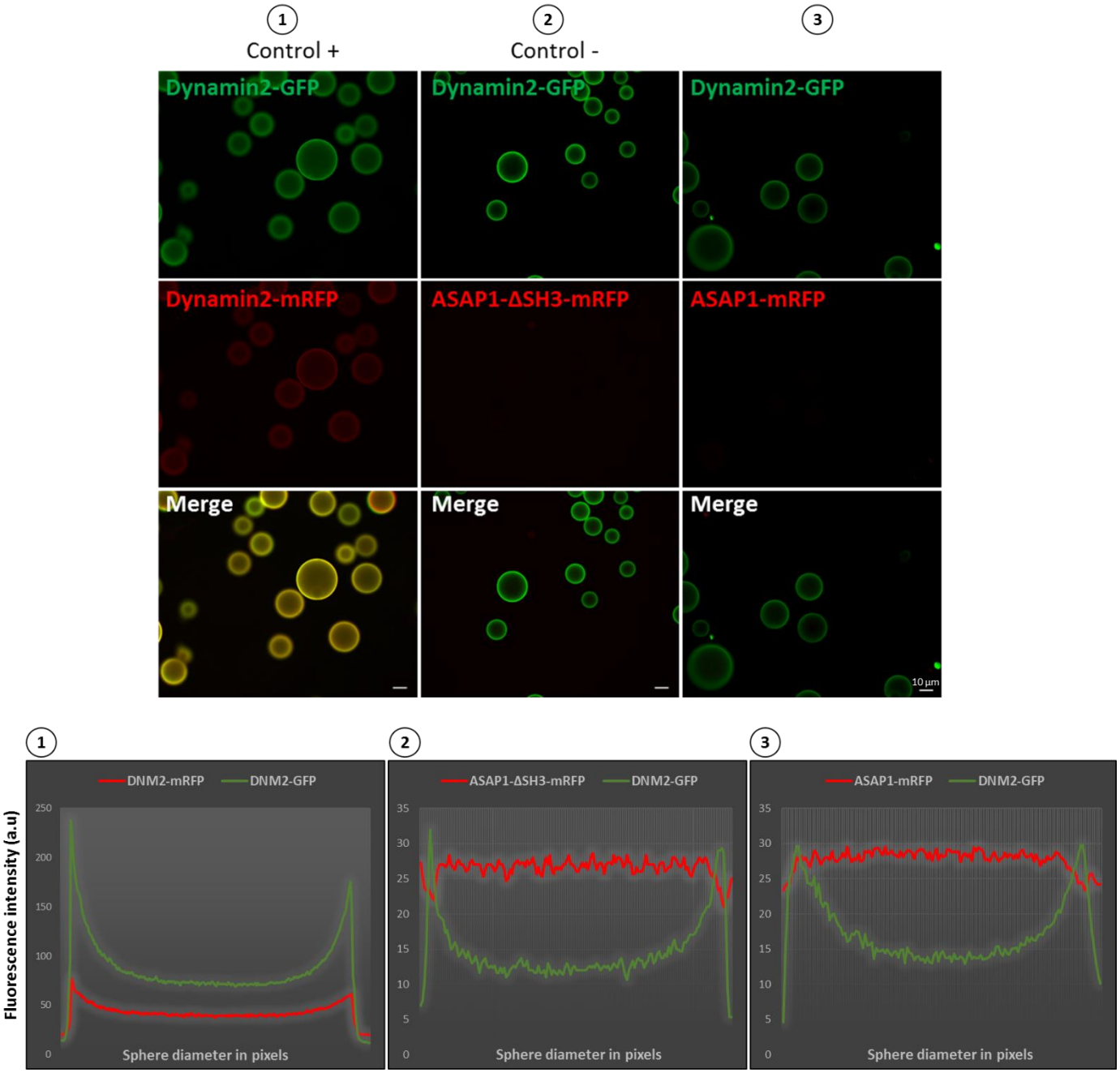

Figure 9: Interaction assay between ASAP1 and Dynamin 2. Visual ImmunoPrecipitation (VIP) assay was performed with GST-nanobody anti GFP beads. Top panel: The positive control was DNM2-GFP coprecipitated with DNM2-mRFP (first column) and analyzed by fluorescent microscopy. As negative control, truncation of the SH3 domain on ASAP1 was used (second column). Unfortunately, the assay doesn't show, for the moment, interaction between DNM2 and ASAP1 (third columns). Bottom panel: The correspondent graphics show the line scanning for fluorescence intensity along the sphere diameter. The first graph shows a correct pattern for interacting proteins with two pics situated on the edge of the sphere. On the contrary, the second and third graphs represent the non-interacting samples, ASAP1-ΔSH3 and ASAP1, with no match of green and red curve.

My last chance to obtain any indication about the nature of interaction between ASAP1 and dynamin 2 in the last period of my internship, was Visual ImmunoPrecipitation (VIP) assay [30]. Using fluorescently tagged proteins (e.g. GFP and mRFP), this assay meant to give a qualitative result in the case of interaction between the two fluorescently tagged proteins. A merged signal (e.g. yellow signal for the combination of GFP and mRFP) can be found by microscopic observation and the final images could be analysed by ImageJ to obtain a fluorescent profile. For this assay, I used the same glutathione-sepharose 4B beads linked to the purified GST- nanobodies anti GFP so that the dynamin 2-GFP would have been strictly linked to the nanobody and I could possibly see the presence of ASAP1-mRFP on the same beads after immunoprecipitation. As a positive control for this experiment I used the well-known interaction between dynamin 2 monomers to form dimers [31]: the monomers of dynamin 2 were fused to either GFP or mRFP and the results of the merged images showed yellow bright colour indicating an interaction between dynamin 2 monomers (Figure 9, top panel, 1). Line scanning of a representative bead showed similar intensity profiles for both dynamin 2-GFP and dynamin 2-mRFP supporting their interaction (Figure 9, bottom panel, 1). As I expected, ASAP1-ΔSH3 showed almost no red signals on the beads (Figure 9, top panel, 2) which was also confirmed by line scanning (Figure 9, bottom panel, 2) suggesting no interaction between these proteins. Unexpectedly, full-length ASAP1 also showed a negative signal on the beads (Figure 9, top panel, 3) with an intensity profile suggesting poor interaction between ASAP1 and dynamin 2 (Figure 9, bottom panel, 3). Despite several attempts, I wasn't able to give any positive results on this subject. I have not collected any clues suggesting possible interaction between ASAP1 and dynamin 2 at this stage, but further experiments such as *in vitro* binding assay using purified proteins may clarify this issue in the future.

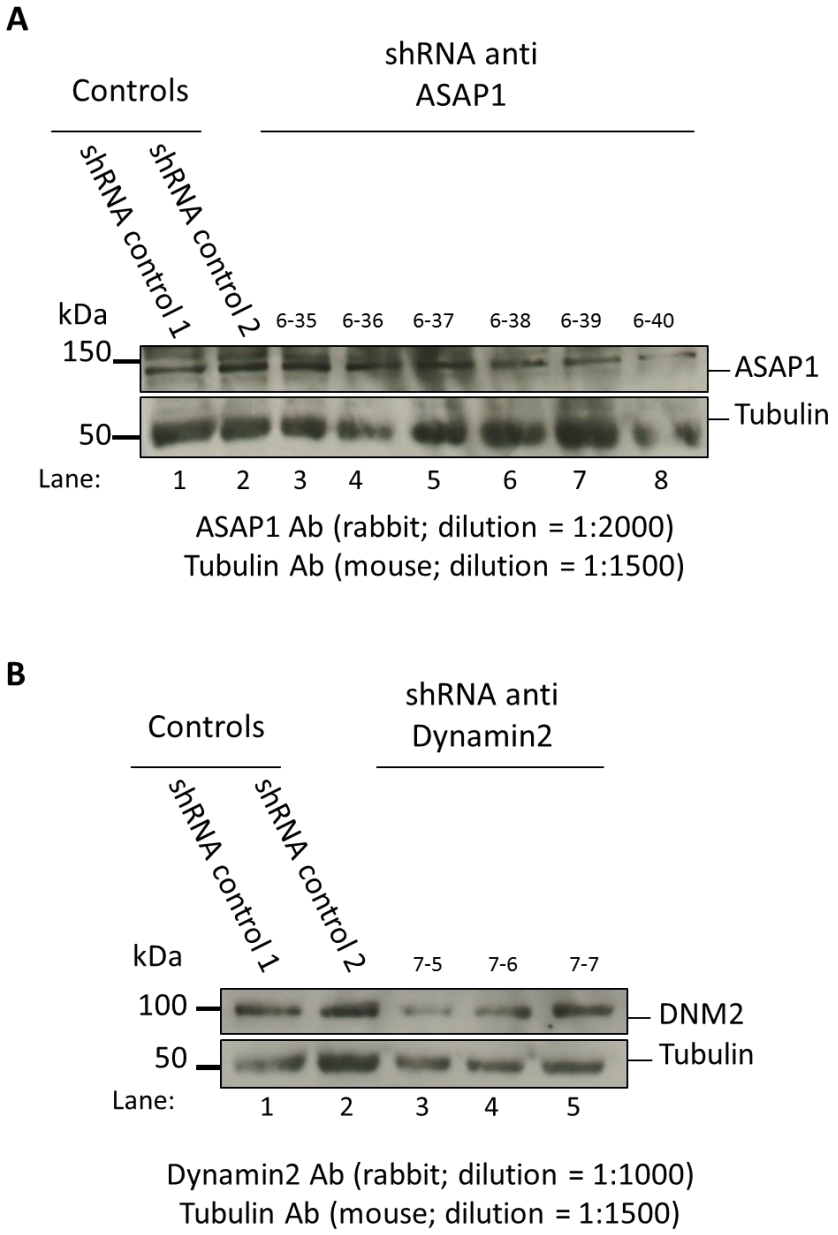

Figure 10: Western blot for stable cell line production. shRNAs were transfected in T24 cells three weeks before the immunoblotting analysis; tubulin is used as internal control. (A) Immunoblotting for ASAP1 using its specific antibody to detect the endogenous protein; controls show the correct expression of the protein without interference. The columns from 3 to 8 show the different shRNA sequences used for this experiment against ASAP1. Only the lane number 8 shows a decreased expression of the endogenous protein. (B) the same controls as above has been used for the KD experiment for Dynamin 2; specific antibody against Dynamin 2 shows a slightly decrease of the expression in the lane number 3.

Elucidate the requirement of ASAP1 for invadopodia function in T24

The last step of my research was to elucidate the requirement of ASAP1 in the invasion process. To do so, I created new stable cell lines expressing different shRNA constructs which should knock down (KD) the corresponding genes in T24. For this experiment, I used two control shRNAs, six shRNAs against ASAP1 and three shRNAs against dynamin 2. I transfected T24 cells with those shRNA constructs in a 24 wells plate and assure the selection process by adding puromycin (selected antibiotic resistant gene). The concentration of puromycin was increased from 0.5 μg/ml up to 30μg/ml during a period of three weeks with repeated changes of medium every 36 hours. The non-transfected cells died the day after the initial addition of puromycin, and the other samples were growing at a lower speed than normal, suggesting that the selection process was being successful. After 14 days from the start of the experiment, I saw a normal growth of the cells and then I tried to boost the final selection by adding higher concentration of puromycin (30 μg/ml) for the entire last week of culture before harvesting and analyze the protein expression level by immunoblotting. The larger concentration of antibiotic didn't affect significantly the ability of the cells to replicate, proving me a well-established presence of the resistant gene inside the cells' genome. After securing the culture splitting the samples in different 24 wells plates, I harvested the colonies and analyzed them by western blot.

The expression level of ASAP1 and dynamin 2 in the stable cell lines expressing respective shRNA was checked by immunoblot analysis (Figure 10). The expression level of ASAP1 in the ASAP1 KD cells was equivalent to that in control cells (Figure 10 A), suggesting inefficient reduction of ASAP1 in KD cells. Only the clone 6-39 showed a slight reduction of ASAP1 (Figure 10 A, lane 8), but it was not a sufficient drop of expression for analyzing ASAP1 KD phenotype.

It was also the case for the dynamin 2 KD cells and only the clone 7-5 showed a slight decrease in its expression level (Figure 10 B, lane 3). Unfortunately, it was my last attempt to analyze these stable ASAP1 KD and dynamin 2 KD cells, since I have got these results during my last week in Japan. The samples from this experiment were eventually frozen and stored in liquid nitrogen for future analyses.

IV. Conclusion and perspectives

In this study, I established an improved version of invadosome induction assay which facilitated microscope imaging (Figure 4). Using this improved assay conditions, I showed for the first time that ASAP1 localizes to the invadopodia together with other invadosomal markers, such as cortactin and actin in T24 cell line (Figure 5). Structure-function analyses of ASAP1 showed that SH3 domain of ASAP1 is dispensable for its invadopodia localization (Figure 6), uncaracterized regions located between BAR domain and SH3 domain may be required for its localization to the invadopodia. As we expected, ASAP1 and dynamin 2 co-localize at the invadopodia (Figure 7) suggesting their cooperative function during cancer invasion.

Unfortunately, despite multiple attempts using different approaches for protein-protein interaction assays, any clues of ASAP1 - dynamin 2 interaction could not be detected (Figure 8 and 9). Future experiments using more direct *in vitro* binding assay may reveal the possible interaction between ASAP1 and dynamin 2. Furthermore, live cell imaging and/or super resolution microscopy of ASAP1 and dynamin 2 will gain new insights into spatial and temporal distribution of these proteins in the invadopodia.

ASAP1 KD stable cell lines that I have established in this study failed to reduce its expression (Figure 10), probably due to adaptation of cells to the lower expression level of ASAP1. To avoid such an adaptation of cells, acute KD using conventional RNAi with siRNA may need be done in the future. Once KD of ASAP1 is confirmed, it would be possible to perform different experiments to analyze its effect on invasiveness of cancer cells. For example, an invasion assay with fluorescent gelatin coated coverslips would be useful to analyze the proteolytic ability of invadopodia after the loss of ASAP1. A trans-well invasion assay could also be a valid test to acquire useful data about changes in migration capacity of cancer cells in the absence of ASAP1.

Future work in the lab would be to elucidate a bigger molecular network surrounding dynamin 2 in the invadopodia to unveil molecular mechanisms of cancer invasion.

V. Bibliography

1) N. V. Krakhmal et al., Cancer Invasion: Patterns and Mechanisms, Acta Naturae; 2015; 7(2): 17–28.
2) Pecorino L. et al.; Molecular Biology of Cancer. Mechanisms, Targets, and Therapeutics. Third ed. 2012; Oxford: Oxford University Press.
3) Pantel K. et al.; Dissecting the metastatic cascade; Nat Rev Cancer; 2004; 4(6):448-56.
4) Hiom SC; Diagnosing cancer earlier: reviewing the evidence for improving cancer survival; Br J Cancer; 2015; 112 Suppl 1:S1-5.
5) D.S. Kaufman et al. ; Bladder cancer; Lancet; 2009; 374: 239-249.
6) S. van den Bosch et al.; Long-term cancer-specific survival in patients with high-risk, non-muscle-invasive bladder cancer and tumour progression: a systematic review, Eur. Urol.; 2011; 60 (3) 493-500.
7) A.P. Mitra, et al., Factors influencing post-recurrence survival in bladder cancer following radical cystectomy; BJU Int.; 2012; 109 (6) 846-854.
8) A.D. Nikapota, et al., Quality of life after bladder Cancer: a prospective study comparing patient-related outcomes after radical surgery or radical radiotherapy for bladder Cancer; Clin. Oncol.; 2016; 28 (6) 373-375.
9) Daisuke Hoshino et al.; Signaling inputs to invadopodia and podosomes; Journal of Cell Science; 2013; 126, 2979–2989.
10) Danielle A. Murphy et al.; The 'ins' and 'outs' of podosomes and invadopodia: characteristics, formation and function; Nat Rev Mol Cell Biol.; 2012; 12(7): 413–426.
11) Jing Y. et al.; New therapeutic targets for cancer bone metastasis; Trends in Pharmacological Sciences; 2015.
12) Yubai Zhang et al.; Dynamin2 GTPase contributes to invadopodia formation in invasive bladder cancer cells; Biochemical and Biophysical Research Communications; 2016; 480: 409-414.
13) S.M. Ferguson, P. De Camilli, Dynamin, a membrane-remodelling GTPase; Nat. Rev. Mol. Cell Biol.; 2012; 13 (2) 75-88.
14) M. Baldassarre et al.; Dynamin participates in focal extracellular matrix degradation by invasive cells; Mol. Biol. Cell; 2003; 14 (3) 1074-1084.

15) H. Yamada, et al.; Actin bundling by dynamin 2 and cortactin is implicated in cell migration by stabilizing filopodia in human non-small cell lung carcinoma cells; Int. J. Oncol.; 2016; 49 (3) 877-886.
16) Megan T. Brown et al.; ASAP1, a Phospholipid-Dependent Arf GTPase-Activating Protein That Associates with and Is Phosphorylated by Src; MOLECULAR AND CELLULAR BIOLOGY; 1998; p. 7038–7051.
17) Minghua Li et al.; ASAP1 mediates the invasive phenotype of human laryngeal squamous cell carcinoma to affect survival prognosis; Oncology Reports; 2014; 31: 2676-2682.
18) Cristina Casalou et al.; Arf proteins in cancer cell migration; Small GTPases; 2016; Vol. 7, No. 4, 270–282.
19) Sanita Bharti et al.; Src-Dependent Phosphorylation of ASAP1 Regulates Podosomes; Molecular and Cellular Biology; 2007; Vol. 27, No. 23 p. 8271–8283.
20) Alissa M. Weaver; Invadopodia: specialized cell structures for cancer invasion; Clin Exp Metastasis; 2006; 23: 97–105.
21) Ziqing Wang et al.; Analysis of invadopodia formation in breast cancer cells; Methods Mol Biol.; 2016; 1406: 203–210.
22) Mihoko Sutoh et al.; Invadopodia Formation by Bladder Tumor Cells; Oncology Research; 2010; Vol. 19, pp. 85–92.
23) Dong Lin et al.; ASAP1, a Gene at 8q24, Is Associated with Prostate Cancer Metastasis; Cancer Res; 2008; 68: 11.
24) Abitha Jacob et al.; The role and regulation of Rab40b–Tks5 complex during invadopodia formation and cancer cell invasion; Journal of Cell Science; 2016; 129: 4341-4353.
25) Yasuhito Onodera et al.; Expression of AMAP1, an ArfGAP, provides novel targets to inhibit breast cancer invasive activities; The EMBO Journal; 2005; 24: 963–973.
26) Ruibai Luo et al.; Arf GAPs and molecular motors; Small GTPases; 2017.
27) Seano G. et al.; Podosomes and invadopodia: tools to breach vascular basement membrane; Cell Cycle; 2015; 14(9): 1370-4.
28) Thomas P. et al.; HEK293 cell line: a vehicle for the expression of recombinant proteins; J Pharmacol Toxicol Methods; 2005; 51(3): 187-200.

29) Solomaha E. et al.; Kinetics of Src homology 3 domain association with the proline-rich domain of dynamins: specificity, occlusion, and the effects of phosphorylation; J Biol Chem.; 2005; 280(24): 23147-56.
30) Yohei Katoh et al.; Architectures of multisubunit complexes revealed by a visible immunoprecipitation assay using fluorescent fusion proteins; Journal of Cell Science; 2015; 128, 2351-2362.
31) Justin A. Ross et al.; Oligomerization State of Dynamin 2 in Cell Membranes Using TIRF and Number and Brightness Analysis; Biophys J.; 2011; 100(3): 15–17.
32) Nicolas Reymond et al.; Crossing the endothelial barrier during metastasis; Nature Reviews Cancer; 2013; 13, 858–870.
33) MBInfo contributors. Invadopodia assembly. In MBInfo Wiki, Retrieved 10/21/2014 from http://mbinfo.mbi.nus.edu.sg/figure/invadopodia-assembly/